Observation of Normal-Mode Splitting for an Atom in an Optical Cavity

R. J. Thompson, G. Rempe, and H. J. Kimble

Norman Bridge Laboratory of Physics 12-33, California Institute of Technology, Pasadena, California 91125

(Received 4 November 1991)

An investigation of the spectral response of a small collection of two-state atoms strongly coupled to the field of a high-finesse optical resonator is described for mean number $\bar{N} \leq 10$ atoms. For weak excitation, a coupling-induced normal-mode splitting is observed even for one intracavity atom, representing a direct spectroscopic measurement of the so-called vacuum Rabi splitting for the atom-cavity system.

PACS numbers: 42.50.Fx, 32.80.−t, 42.65.Pc

Much of modern research in optical physics has as its cornerstone the interaction Hamiltonian describing the dipole coupling of a "two-state" atom to the electromagnetic field. In the preponderance of cases, as in the usual theories of the laser [1,2], of resonance fluorescence [3], and of optical bistability [4], the atom-field interaction can be described in a regime of weak coupling, for which the rate β for irreversible decay into the continuum of degrees of freedom of the electromagnetic field is much larger than the frequency scale g associated with reversible evolution in the interaction of any one mode of the field with the atom. Although weakly coupled systems can be strongly driven to produce coherent excitation with characteristic frequency $\chi \gg \beta$ (with χ proportional to the amplitude of excitation), the system remains weakly coupled in that the interaction frequency g for a single quantum is negligible. Note that χ becomes $g\sqrt{n}$ in the limit that the coupling frequency $g \rightarrow 0$ and the number of quanta $n \rightarrow \infty$.

In contrast to this usual circumstance of weak coupling, recently it has become possible in research in the area of cavity quantum electrodynamics [5] to achieve a situation of strong coupling for which $g > \beta$ and for which a photon emitted by an atom into a cavity mode is likely to be repeatedly absorbed and reemitted before irreversibly escaping into the environment [6–8]. This oscillatory exchange of excitation between atom and cavity mode arises from a ubiquitous normal-mode splitting in the eigenvalue spectrum of the interaction Hamiltonian for the strongly coupled system which was described long ago by Jaynes and Cummings [9] for a single intracavity atom ($N=1$) and by Tavis and Cummings [10] for $N > 1$. Although Jaynes-Cummings dynamics have been investigated for $N=1$ and a few photons [6b], and while mode splittings have been studied previously for $N \gg 1$ [11–14] and quite recently for $N \simeq 3$ [15], apparently the so-called vacuum Rabi splitting [16,17] of the first excited state for a single atom coupled to a cavity mode has not been similarly observed. With this backdrop, we report in this Letter an optical experiment where the weak-field normal-mode splitting for an atom-cavity system is investigated by direct spectroscopic measurements. In particular, for the case of average intracavity atomic number $\bar{N} \simeq 1$, we record the response of the system to a variable-frequency input probe and observe a distinctive doublet symmetrically split by $\pm g$ about the otherwise common resonance frequency of atom and cavity. Because our measurements are carried out in an atomic-beam apparatus with fluctuations both in the number of atoms within the cavity-mode volume and in the atomic spatial positions, we present results from numerical simulations which extend the standard theory to approximate our situation. The agreement between this extended theory and the measured spectral responses is quite good and substantiates our observation of the normal-mode or vacuum Rabi splitting for a single intracavity atom.

Our investigation of the structure of the atom-cavity system is restricted to a regime of weak excitation and consequently equivalent descriptions follow either from the quantum master equation or from the semiclassical Maxwell-Bloch equations, since in this domain the system behaves as coupled linear oscillators. Quantum mechanically the basis is limited to states with only zero or one quantum of excitation so that the coupling-induced splitting of the first excited state of the Jaynes-Cummings "molecule" is probed, while semiclassically the intracavity intensity is held much smaller than the saturation intensity so that the linear susceptibility of the composite entity is probed. In either case the response of the system is given in terms of the eigenvalues for the normal modes, which are of course independent of the particular excitation scheme and initial conditions. Our choice is to measure the steady-state transmission function $T(\omega_p)$ for a weak external probe field of variable frequency ω_p. $T(\omega_p)$ is found from the ratio of transmitted (P_o) to incident (P_i) power, and for the case of coincident cavity ω_C and atomic ω_A frequencies is given by [4,17]

$$T(\omega_p) = T_0 \left| \frac{\kappa[\gamma_\perp + i(\omega_0 - \omega_p)]}{(\omega_p - \lambda_+)(\omega_p - \lambda_-)} \right|^2 , \qquad (1)$$

where T_0 is the peak transmission of the empty cavity and κ is the cavity-field decay rate. Since the solid angle for our cavity mode is small ($\sim 10^{-4}$ sr), the rates $(\gamma_\perp, \gamma_\parallel)$ for the decay of the atomic polarization and inversion are as in free space, with $\gamma_\parallel = 2\gamma_\perp = \frac{1}{32}$ ns. The eigenvalues $\lambda_\pm$ describe the (collective) normal modes formed from the "cavity-field oscillator" and the "atomic-polarization oscillator" and are given by $\lambda_\pm = (\omega_0 \pm \Omega_0) - i(\gamma_\perp + \kappa)/2$, with $\omega_C = \omega_A \equiv \omega_0$ and the frequency $\Omega_0 \equiv [g_0^2 N - (\gamma_\perp - \kappa)^2/4]^{1/2}$ specifying a nor-

© 1992 The American Physical Society

mal-mode splitting for $g_0\sqrt{N} > |\gamma_\perp - \kappa|/2$. The dipole coupling coefficient for an atom of transition moment μ at site $\mathbf{r}$ in our TEM_{00} standing-wave cavity is $g(\mathbf{r}) \equiv g_0\psi(\mathbf{r})$, where $g_0 \equiv (\mu^2\omega_C/2\hbar\epsilon_0 V)^{1/2}$ is the optimum coupling coefficient and $\psi(\mathbf{r}) = \sin kz \exp[-(x^2 + y^2)/w_0^2]$ is the cavity-mode function with mode volume $V = \pi w_0^2 l/4$. For a distribution of atoms at different sites $\mathbf{r}_j$, the effective intracavity atomic number $N \equiv \sum_j |\psi(\mathbf{r}_j)|^2$.

Turning now to the experimental procedure for recording $T(\omega_p)$, we generate the frequency-tunable probe beam from the output of a frequency-stabilized titanium-sapphire laser (60 kHz rms linewidth) by acousto-optic and electro-optic modulators (Fig. 1). By employing an auxiliary vapor cell, the primary, unshifted output frequency ω_L of the laser is locked and independently tunable relative to the frequency ω_A of the $(6S_{1/2}, F=4, m_F=4) \rightarrow (6P_{3/2}, F'=5, m_F'=5)$ transition of the D_2 line of cesium in the atomic beam. The resonance frequency ω_C of a TEM_{00} longitudinal mode of the spherical mirror cavity formed by the mirrors M_i and M_o is locked to ω_L with a chopping technique that alternates between, on the one hand, data collection with the probe beam at ω_p switched "on" and directed by the acousto-optic modulator (AOM) to detector D1 and, on the other hand, cavity stabilization with the intense locking beam at ω_L switched "on" and directed to D2. The stabilization of ω_C to ω_L and locking of ω_L relative to ω_A are such that all detunings are zero to within ± 0.2 MHz. Other parameters for our system are cavity finesse $F = 8\times10^4$, mode waist $w_0 = 50$ μm, cavity length $l = 1$ mm, and atomic-beam size (0.3,3) mm along (z,y). The fundamental rates appearing in Eq. (1) are $(g_0, \gamma_\perp, \kappa) = [2\pi(3.2\pm0.2, 2.5\pm0.2, 0.9\pm0.1)]$ MHz, with g_0 calculated from its definition and as well determined from the measured saturation photon number $n_0 \equiv 2\gamma_\perp\gamma_\parallel/3g_0^2$ for our system [8].

In Fig. 2 we display a series of transmission spectra $T(\Omega)$, where $\Omega \equiv \omega_p - \omega_0$ and T is normalized in units of mean intracavity photon number $\bar{n}$. Clearly evident in each of the traces (a)-(d) are two peaks which are symmetrically split about the frequency $\omega_p = \omega_0$ and

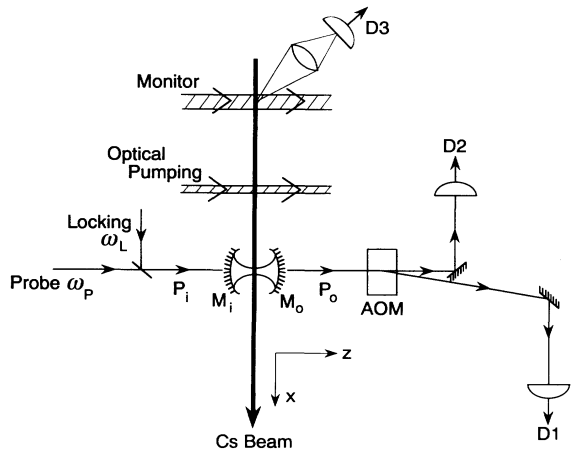

FIG. 1. Diagram of principal elements of the experiment.

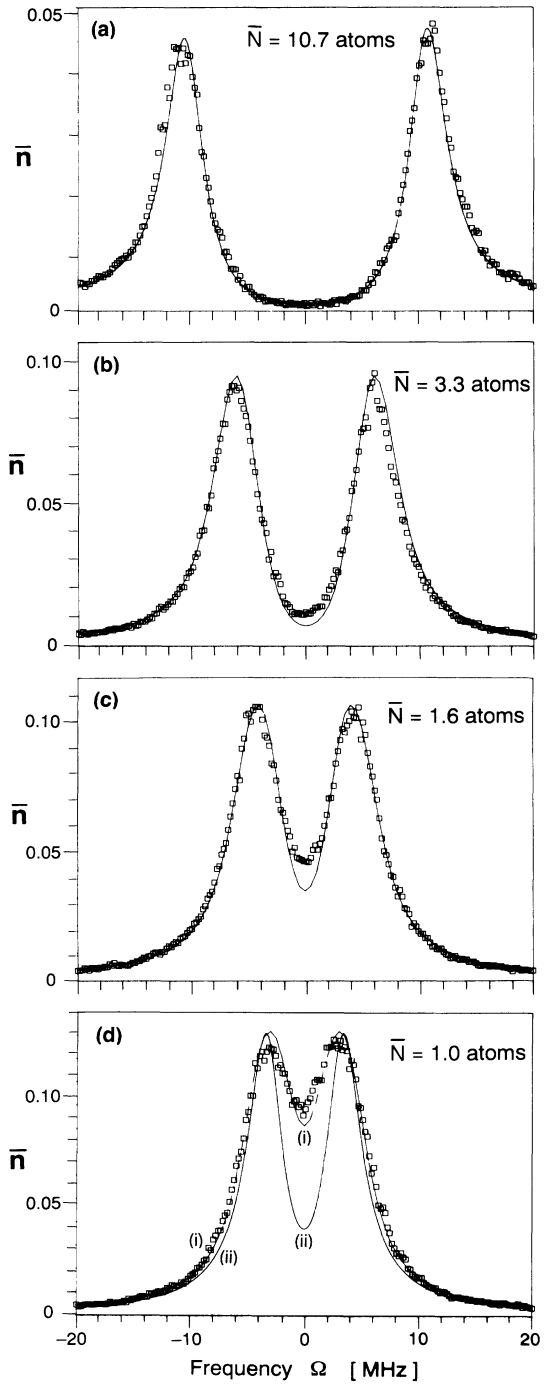

FIG. 2. Intracavity photon number $\bar{n}$ vs probe frequency Ω for four values of $\bar{N}$ and with $\omega_C \simeq \omega_A$. Curves in (a)-(c) and curve i in (d) are theoretical fits to the data including fluctuations in atomic number and position. Curve ii in (d) is from Eq. (1) for a single intracavity atom with optimum coupling g_0.

which reflect the weak-field normal-mode splitting $\pm\Omega_0$ for the atom-cavity system. Over a wide range, these experimental spectra are independent of the field amplitude and hence represent the weak-field, linear response. Also shown in the figure as solid curves are fits to the experimental spectra obtained from Eq. (1) with the measured values g_0, $\gamma_\perp$, and κ. In calculating the fits, a numerical simulation has been employed to place N' atoms randomly over positions in a volume $V' \gg V$. For each particular random toss of atoms into V', an individual spectrum is evaluated from Eq. (1) by summing over the resulting atomic sites $\mathbf{r}_j$, with coupling specified by $\psi(\mathbf{r}_j)$ and with the mean number of atoms in V over many trials given by $\bar{N} \equiv \langle \sum_j |\psi_j|^2 \rangle \ll N'$. The average of a large number of such spectra is then taken to approximate the experimental spectra, which involve fluctuations both in atomic number and in atomic position from the intersection of the atomic beam with the cavity-mode function. Note that transit-time effects have not been included in our model. Numerical integrations of the Maxwell-Bloch equations for atomic trajectories through the cavity mode indicate that the effects of transit are small since the damping rate $(\gamma_\perp + \kappa)/2$ is larger than the inverse atomic transit time $\tau_t = 4 \times 10^{-7}$ s. In fitting the theory to the experiment, we stress that the only adjustable parameter is $\bar{N}$; values of $\bar{N}$ determined from the fits are indicated for each trace in Figs. 2(a)–2(d). In each case the resulting values of $\bar{N}$ agree quite well with a much more straightforward determination based upon the frequency separation 2Δ of the peaks; that is, $\bar{N} = \Delta^2/g_0^2$.

Although the quality of the theoretical fits in Fig. 2 is good, clearly the accurate determination of $\bar{N}$ for our spectra is of crucial importance. Additional measurements to address this question are presented in Fig. 3, where the values of $\bar{N}$ found from fits to a number of spectra as in Fig. 2 are displayed against the corresponding values of the fluorescence F of a monitor beam collected with detector D3 as shown in Fig. 1. The monitor fluorescence serves as a proportional measure of the density of the atomic beam, with the constant of proportionality calculated from those spectra which display well-resolved splittings and for which fluctuations in N play a minor role. The appropriateness of this procedure and indeed of the basic theory of Eq. (1) to an experiment such as ours has been previously established in absolute measurements of the system eigenvalues over the range $20 \leq \bar{N} \leq 600$ with no adjustment of $\bar{N}$ [13]. Hence while the monitor fluorescence certainly serves to calibrate ratios of density, the work of Ref. [13] provides a bridge so that it can also be used for the absolute determination of $\bar{N}$ when $\bar{N}$ is large. The good correlation between $\bar{N}$ and F evidenced in Fig. 3 over the whole range of atomic density, and in particular in the region where the two peaks of the spectra begin to merge together, lends strong support to our procedure of finding $\bar{N}$ from fits to the experimental spectra, which relies only upon the independently derived values of g_0, $\gamma_\perp$, and κ.

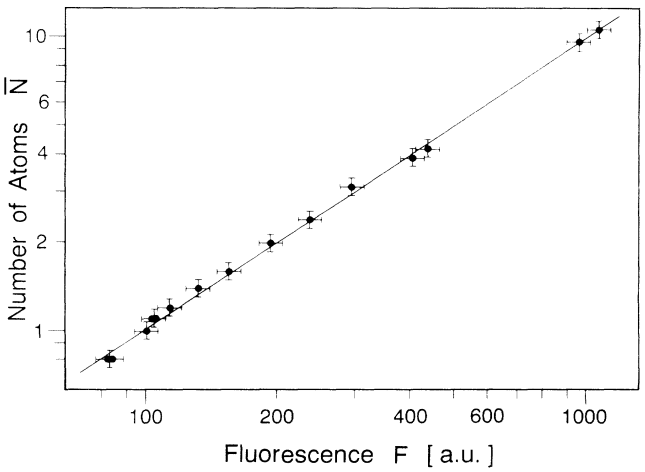

FIG. 3. Average number of atoms $\bar{N}$ vs monitor fluorescence F. The straight line connects the origin with the two highest points.

A somewhat different approach to the problem of determining $\bar{N}$ is to make a virtue rather than a vice of the fluctuations inherent in the atomic beam. In particular, note that the distribution of fluctuations for the number and positions of the intracavity atoms itself depends upon $\bar{N}$. Thus the spectrum which arises for a particular value of $\bar{N}$ will contain signatures that are unique to that value of $\bar{N}$ through the dependence on the associated fluctuations. For $\bar{N} \sim 1$, these signatures can be quite distinctive, as we illustrate in Fig. 4(a). Shown in the figure is a measured spectrum with the best theoretical fit (curve i) corresponding to $\bar{N} = 1.1$. Also displayed are two curves for which $\Omega_0 \simeq g_0 \bar{N}^{1/2}$ remains fixed, but for which $\bar{N}$ has been adjusted slightly downward (curve ii, $\bar{N} = 0.9$) or upward (curve iii, $\bar{N} = 1.3$), with the changes in $\bar{N}$ corresponding to changes in g_0 at the limits of our experimental uncertainty. The obvious degradation in the quality of the fit around $\Omega = 0$ reflects the fact that the spectra in this region are very sensitive to atomic fluctuations and hence to the precise value of $\bar{N}$. By contrast, in the absence of fluctuations in the number or positions of the intracavity atoms, spectra obtained directly from Eq. (1) would be indistinguishable under the scaling $N \rightarrow s^2 N$, $g \rightarrow g/s$, with Ω_0 constant. Thus the behavior of the spectra around $\Omega = 0$ provides a self-calibration of $\bar{N}$ through a sensitive dependence on the intracavity atomic fluctuations.

With $\bar{N}$ determined by way of the avenues described above, there remains the question of identifying specific contributions to the measured spectra from atoms at different mode sites. Of particular relevance to the current discussion is the case $\bar{N} \simeq 1$, for which we wish to assess the contribution from a single atom in the mode volume. Towards this end, we present in Fig. 2(d) both the theoretical spectrum obtained by averaging over atomic number and position ($\bar{N} = 1$, curve i) and the simple result from Eq. (1) for a single, optimally coupled

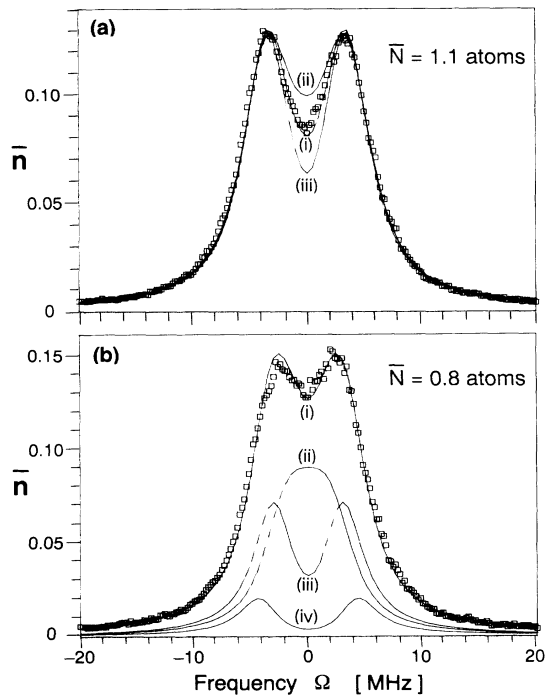

FIG. 4. Intracavity photon number $\bar{n}$ vs probe frequency Ω with $\omega_C \simeq \omega_A$. (a) Normal-mode splitting for $\bar{N} \simeq 1$ atom with three theoretical fits to illustrate the sensitivity of the spectra to fluctuations in N and hence to $\bar{N}$ itself. For curves i–iii $g_0\bar{N}^{1/2}$ is held constant while g_0 and $\bar{N}$ are individually varied: curve i, $g_0 = 2\pi \times 3.2$ MHz, $\bar{N} = 1.1$; curve ii, $g_{0+} = 2\pi \times 3.5$ MHz, $\bar{N} = 0.9$; curve iii, $g_{0-} = 2\pi \times 2.9$ MHz, $\bar{N} = 1.3$. g_0 is the measured value while $g_{0\pm}$ are at the limits of the experimental uncertainty. (b) Normal-mode splitting for $\bar{N} \simeq 0.8$ atom with theoretical fit (curve i). Curves ii–iv show the contributions to curve i from the cases with zero atoms in the mode-volume V (curve ii), with precisely 1 atom in V (curve iii), and with two or more atoms in V (curve iv).

atom [$N = 1$, $g(\mathbf{r}) = g_0$, curve ii]. It should be reasonably clear that a dominant contribution to the measured spectrum arises from the single-atom, optimum-coupling result (curve ii). That there is a small reduction of splitting in curve i relative to curve ii is certainly to be expected since a single atom is likely to be found not only at the peak of the mode function [for which $\psi(\mathbf{r}) = 1$], but can as well be located at sites with smaller coupling coefficients. These qualitative considerations are made more quantitative in Fig. 4(b), where a measured transmission spectrum is displayed together with the theoretical best fit ($\bar{N} = 0.8$, curve i). As previously discussed, this theoretical result is the average of many spectra, each of which is computed from a trial with a random toss of atoms into the simulation volume V'. These individual trials can be sorted into various classes, with curve i as the sum over all classes. In particular curve ii in Fig. 4(b) is the contribution from the class of trials in the simulation with zero atoms in V [but of course with atoms with coupling $|\psi(\mathbf{r})|^2 \leq 0.33$ in the tails of the mode function extending into $V' \gg V$]; curve iii is the class of trials with one and only one atom in the mode volume [with $|\psi(\mathbf{r})|^2 > 0.33$]; and curve iv is the sum of all remaining trials which include the contributions from two or more atoms in the mode volume. Apparently then the splitting displayed in the data of Fig. 4(b) (for which curve i provides a good accounting) arises predominantly from individual cases for which a single atom resides in the mode volume. We thus assert that the measurements of Figs. 2(d), 4(a), and 4(b) represent a conclusive observation of the weak-field normal-mode splitting for a single two-state atom in an optical cavity.

Relative to other work in quantum optics, the experiment described in this Letter is distinct in having achieved the operating conditions $g_0 > (\kappa, \gamma_\perp) \gg 1/\tau_t$. Hence the features that we have observed are associated primarily with steady states established by individual atoms rather than with states reached incrementally by the successive passage of large numbers of atoms. Although g_0 is only marginally larger than κ and $\gamma_\perp$ in our current system, the extension of our techniques to smaller cavities with finesse in excess of 10^6 [18] should lead to a variety of possibilities for nonlinear spectroscopic investigations of the structure and dynamics of the atom-cavity system or of the Jaynes-Cummings "molecule."

This work was supported by the NSF (Grant No. PHY-9014547), the ONR (Grant No. N00014-90-J-1059), and Venture Research International, and by a Robert A. Millikan Fellowship (G.R.). We gratefully acknowledge the assistance of Q. Turchette.

[1] H. Haken, *Laser Theory* (Springer-Verlag, Berlin, 1984).
[2] M. Sargent, III, M. O. Scully, and W. E. Lamb, Jr., *Laser Physics* (Addison-Wesley, Reading, MA, 1974).
[3] B. R. Mollow, in *Progress in Optics*, edited by E. Wolf (Elsevier, New York, 1981), Vol. 19, p. 3.
[4] L. A. Lugiato, in *Progress in Optics*, edited by E. Wolf (Elsevier, New York, 1984), Vol. 21 , p. 69.
[5] E. A. Hinds, *Advances in Atomic, Molecular, and Optical Physics*, edited by D. Bates and B. Bederson (Academic, New York, 1990), Vol. 28, p. 237.
[6] (a) D. Meschede *et al.*, Phys. Rev. Lett. **54**, 551 (1985); (b) G. Rempe *et al.*, Phys. Rev. Lett. **58**, 353 (1987).
[7] M. Brune *et al.*, Phys. Rev. Lett. **59**, 1899 (1987).
[8] G. Rempe *et al.*, Phys. Rev. Lett. **67**, 1727 (1991).
[9] E. T. Jaynes and F. W. Cummings, Proc. IEEE **51**, 89 (1963).
[10] M. Tavis and F. W. Cummings, Phys. Rev. **170**, 379 (1968).
[11] Y. Kaluzny *et al.*, Phys. Rev. Lett. **51**, 1175 (1983).
[12] R. J. Brecha *et al.*, J. Opt. Soc. Am. B **3**, 238 (1986).
[13] M. G. Raizen *et al.*, Phys. Rev. Lett. **63**, 240 (1989).
[14] Y. Zhu *et al.*, Phys. Rev. Lett. **64**, 2499 (1990).
[15] F. Bernardot *et al.*, Europhys. Lett. **17**, 33 (1992).
[16] J. J. Sanchez-Mondragon *et al.*, Phys. Rev. Lett. **51**, 550 (1983).
[17] G. S. Agarwal, Phys. Rev. Lett. **53**, 1732 (1984).
[18] G. Rempe *et al.*, Opt. Lett. (to be published).